

## Liquid Spray Morphological Information from Laser-Diffraction Measurements

C. Dumouchel<sup>\*1</sup>, S. Grout<sup>1</sup>, B. Leroux<sup>2</sup> and X. Paubel<sup>2</sup>

<sup>1</sup>CNRS UMR 6614 – CORIA, Université de Rouen  
76801 Saint Etienne du Rouvray, France

<sup>2</sup>Air Liquide, Centre de Recherche Claude Delorme  
78354 Jouy-en-Josas Cedex, France

### Abstract

The Laser-Diffraction Technique (LDT) based on the analysis of the light diffraction pattern forwardly scattered by droplets going through a laser optical probe, reports a drop-diameter distribution of a set of spherical drops that would scatter the same diffraction pattern as the one recorded. However, a light diffraction pattern depends on the shape of the scattering drops. Thus, LDT measures an equivalent diameter distribution that depends on the shape of the drops but the relationship between the equivalent diameter and the actual particle shape is unknown. The experimental investigation presented in this paper addresses this point. The approach consists in measuring liquid spray characteristics with a LDT instrument and an Image Analyzing Technique (IAT). This technique measures the projected area diameter distribution as well as the scale-distribution of the liquid sprays, the latter being explicitly a function of the shape of the drops. All experimental precautions are taken to validate the protocol. The results clearly evidence an influence of drop shape of LDT distribution. The analysis and comparison of the measurements demonstrate that the mean-diameter series of the LDT equivalent-diameter distribution contains information on the drop shapes. Although this result has not been fully explained, it is believed that this performance demonstrates that LDT provides a multi-scale description of the spray droplets. This point is supported by the fact that scale-distribution of the LDT diameter-distribution is very similar to the actual spray scale-distribution inducing the idea that LDT measurement conserves the spray surface-based scale-distribution. These results evidence LDT potentialities that have not been explored so far.

---

### Introduction

The Laser-diffraction technique (LDT) is an optical diagnostic that measures a drop-diameter distribution of liquid sprays evolving in a gaseous environment. This instrument is widely used in research activities dedicated to liquid atomization and sprays. The LDT working principle has been described in many references (see [1, 2] for instance). The light forward scattered by a liquid spray that goes through a cylindrical laser beam is focused by a Fourier lens on a series of diodes that records the light diffraction pattern. A mathematical inversion procedure calculates the volume-based drop-diameter distribution of a set of spherical drops that has the same diffraction pattern as the one recorded. The fact is that any drops going through the optical probe is measured, whatever its shape. Thus, the LDT measurement reports an equivalent-diameter distribution [2]. Indeed, as demonstrated by Borovoi et al. [3] who calculated forward diffraction pattern of non spherical objects, the light diffraction pattern is a function of the shape of the scattering element. Furthermore, by simulating LDT measurements of elliptic objects, Mühlenweg and Hirleman [4] clearly evidenced a dependency between LDT equivalent-diameter distribution and shape of the scattering objects. However, experimental evidency of this dependency has never been reported and the relationship between the LDT equivalent-diameter and the actual droplet shape is unknown and often difficult to determine [2]. This is the objective of the present work.

It is intended in this work to provide experimental evidences of the influence of the drop-shapes on LDT distribution, to propose a better identification of the LDT drop-diameter distribution and to find drop-shape information in LDT drop-diameter distributions. To achieve this, a series of liquid sprays are measured with two diagnostics: a LDT (Spraytec 1997) and an Image Analyzing Technique (IAT). The Image Analyzing Technique is used to measure an equivalent drop-diameter distribution as well as the surface-based scale distribution. Recently introduced to characterize liquid sprays [5], the surface-based scale distribution, summarized in the next section, is explicitly dependent on the shape of the droplets. The comparison between the results obtained with the two diagnostics allows the objectives of the work to be fulfilled.

---

<sup>\*</sup>Corresponding author: [Christophe.Dumouchel@coria.fr](mailto:Christophe.Dumouchel@coria.fr)

### The Surface-Based Scale Distribution

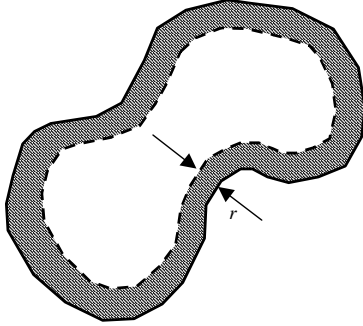


**Figure 1.** Description at scale  $r$  of an object of any shape

A detailed definition of the surface-based scale distribution is available in Dumouchel et al. [5]. This section summarizes this definition and introduces the main characteristics of this distribution. Instead of attributing a single characteristic length to each droplet as done by the traditional drop-diameter distribution, the scale distribution provides a multi-scale description of each element as follows. Let us consider a 2D image containing  $N$  objects of any shape as the one illustrated in Fig. 1. Each object on the image is described as follows. We consider the line defined by the inner point located at a given distance  $r$  from the boundary of the object (see Fig. 1). For each distance  $r$ , called the observation scale, the delimited surface  $S(r)$  (gray surface in Fig. 1) is calculated. When the observation scale covers the whole object, the delimited surface  $S(r)$  is equal to the object total surface area  $S_T$  and the delimited surface  $S(r)$  is kept equal to  $S_T$  for any greater observation scale. For the set of  $N$  objects, the cumulative surface-based scale distribution  $S(r)$  is defined by:

$$S(r) = \frac{\sum_{i=1}^N S_i(r)}{\sum_{i=1}^N S_{T_i}} \quad (1)$$

The first derivative of the cumulative surface-based scale distribution is called the surface-based scale distribution and is noted  $s(r)$  in the following. As for the traditional drop-size distribution, the dimension of the function  $s(r)$  is equal to the inverse of a length. In the following the observation scale  $r$  is replaced by the parameter  $D = 2r$ . (Thus, the observation scale that allows a circular object to be fully covered is equal to its diameter.) The advantage of this distribution compared to the traditional drop-diameter distribution is that the scale-distribution explicitly depends on the shape of the drops (see [5]). Sets of droplets having the same projected-area diameter distribution have different scale distribution if the shape of the droplets is different.

The surface-based scale distribution  $s(D)$  is a continuously decreasing function showing a maximum at  $D = 0$ . This maximum is a measure of the amount of interface length: it is equal to half of the liquid-gas interface length per unit liquid surface area. Examples of this function can be found in [5] and [6]. As done for the traditional diameter-distribution, we define a mean-scale series  $Ds_n$  by the relation:

$$(Ds_n)^n = \int_0^\infty s(D) D^n dD \quad (2)$$

where  $n$  is an integer. Furthermore, it is possible to calculate a shape-parameter series  $PF_n$  by the relation:

$$PF_n = \left[ \frac{(n+1)(n+2)}{2} \right]^{-\frac{1}{n}} \frac{Ds_n}{D'_{n+2,2}} \quad (3)$$

where  $D'_{n+2,2}$  is the mean-diameter series of the equivalent-diameter  $D'$  distribution. For each droplet this equivalent-diameter is the diameter of the circle that has the same surface area of the droplet. (This diameter is sometimes called the projected area diameter [2].) If all drops are circular, the shape parameters  $PF_n$  are all equal to 1 whatever  $n$ . Otherwise, the shape parameters are less than 1 and depend on  $n$ . Therefore, for set of circular drops, Eq. (3) indicates that the mean-diameter  $D'_{32}$  is equal to three time the first order mean-scale  $Ds_1$ , i.e.,  $D'_{32} = 3 Ds_1$ .

### Experimental Setup and Diagnostics

The sprays analyzed in this study are produced by triple disk nozzles (Fig. 2-a and b). The liquid enters disk 1, flows through disk 2 and issues from the nozzle through the decentred single discharge orifice in disk 3. As soon as

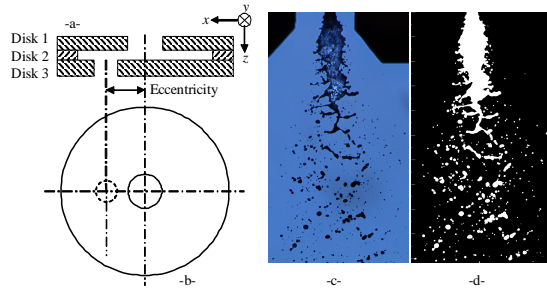


**Figure 2.** a – Side view of the injector and coordinate system, b – Top view of the injector, c – Image of the issuing liquid flow, d – Two-gray level image

**Table 1.** Dimensions of the injectors ( $\mu\text{m}$ )

	Inj. 1	Inj. 2
Disk 1 thickness	177	400
Disk 1 orifice diameter	300	600
Disk 2 thickness	50	100
Disk 2 orifice diameter	2,254	4,510
Disk 3 thickness	76	150
Disk 3 orifice diameter	180	400
Eccentricity	225	450

an illustration, Fig. 2-d shows the two-gray level image of image shown in Fig. 2-c. The details of the treatments required to produce the two-gray level images are available in [3]. The important information to be specified for the present work is that all droplets with an equivalent diameter  $D'$  less than  $17.5 \mu\text{m}$  were removed from the images. The two gray level images are analyzed to measure the surface-based equivalent diameter  $f_s(D')$  and the cumulative surface-based scale distribution  $S(D)$  as well as its first derivative  $s(D)$ . For each operating condition it was demonstrated that the treatment of 25 images was sufficient to obtain statistically representative distributions. As mentioned above, the scale distribution  $s(D)$  is a monotonously decreasing distribution, i.e., it shows a maximum when  $D = 0$ . However, the smallest scale at which  $s(D)$  is determined is  $D = 4$  pixels. This limitation affects the determination of the mean-scale series since the distribution  $s(D)$  is maximum at  $D = 0$ . To avoid this problem, the distribution  $s(D)$  is extended to the scale space origin by using the fact that the slope of  $s(D)$  at  $D = 0$  is equal to  $-2/D'_{20}{}^2$  and is constant over a limited scale-interval whatever the situation. This characteristic feature of the surface-based scale distribution was demonstrated in [5]. The extension procedure consists in imposing the slope  $-2/D'_{20}{}^2$  to the range of scales uncovered by the Image Analyzing Technique. The reliability of this extension procedure is controlled by checking the normalization of the distribution  $s(D)$ . For each operating condition, the normalization was satisfied by 3 % which validated the extension procedure.

The laser-diffraction equipment Spraytec 1997 from Malvern is also used. This diagnostic is equipped with a 10 mm diameter laser beam. The center of this beam is positioned at 20 mm from the nozzle exit. Therefore, the image field and the laser diffraction instrument cover the same region of the spray. Furthermore, these two diagnostics perform a spatial sampling of the spray. We are therefore in the best situation to perform comparison between the results provided by the two diagnostics. In order to avoid confusion in the following, the equivalent-diameter reported by the Laser Diffraction Technique is noted  $\delta$ . The Spraytec instrument provides the volume-based drop-size distribution  $f_v(\delta)$  of the set of spherical droplets that would produce the same diffraction pattern as the one recorded. It can be demonstrated that for such system, the surface-based diameter distribution  $f_s(\delta)$ , the cumulative scale distribution  $S(D)$  and the scale distribution  $s(D)$  are given by (see [5] for details):

the liquid issues from the nozzle, the flow is stretched in the  $x$  direction and forms a sheet whose edges are perturbed. Some of these perturbations grow and the liquid flow rearranges as a liquid ligament network that eventually atomizes as a cloud of drops (Fig. 2-c). The field covered by the image is equal to  $10.5 \times 7 \text{ mm}^2$ . The behavior of such nozzles was fully detailed in a previous article [7]. In the present investigation, two triple nozzles are used. Their dimensions are reported in Table 1. Note that the dimensions of Inj. 2 are twice those of Inj. 1.

Throughout the investigation a single fluid is used (water). The injection pressure varies according to the injector. For Inj. 1, it ranges from 2.5 to 5 bar and for Inj. 2 it covers the interval 2 to 20 bar. The range of gaseous Weber numbers (based on air density and discharge orifice diameter) is equal to  $[0.6; 1.3]$  and to  $[1.4; 14]$  for Inj. 1 and 2, respectively. The range of Reynolds number of the issuing liquid flow is equal to  $[2500; 3600]$  and to  $[5600; 17600]$  for Inj. 1 and 2, respectively.

Shadowgraph images of the sprays are taken with a high-resolution camera ( $2,016 \times 3,040 \text{ pixel}^2$ ) and a short light source (11 ns). The images cover the same field as those shown in Fig. 2-c which corresponds to a spatial resolution equal to  $3.47 \mu\text{m}/\text{pixel}$ . The middle pixel line of the image is located at 20 mm from the nozzle exit section, i.e., beneath the image shown in Fig. 2-c. An image treatment is applied to produce two-gray level images where the liquid appears in white and the background in black. As

$$\begin{cases} f_s(\delta) = \frac{\delta_{32}}{\delta} f_v(\delta) \\ S(D) = F_s(D) + \frac{D}{\delta_{20}^2} [2\delta_{10}(1 - F_l(D)) - D(1 - F_n(D))] \\ s(D) = \frac{2}{\delta_{20}^2} [\delta_{10}(1 - F_l(D)) - D(1 - F_n(D))] \end{cases} \quad (4)$$

where  $\delta_{pq}$  are the traditional mean diameters and  $F_s$ ,  $F_l$  and  $F_n$  the traditional surface-based, length-based and number-based cumulative diameter distributions, respectively. Finally, as the Image Analyzing Technique doesn't detect droplets with an equivalent diameter less than  $17.5 \mu\text{m}$ , it was decided to remove from the diameter distribution reported by the Spraytec all diameter less than this limit and to renormalize the distribution. By taking this precaution, we make sure that both diagnostics analyze the same drop categories.

## Results

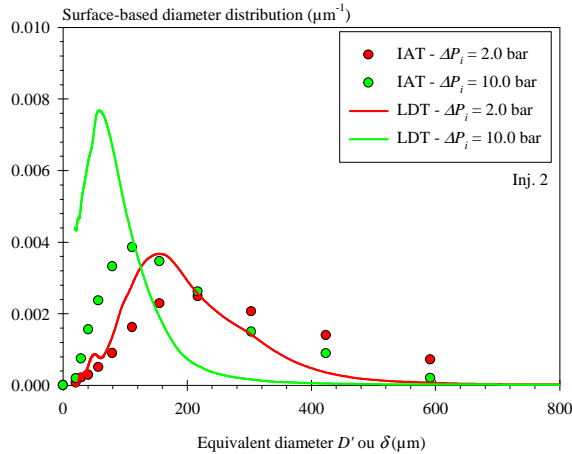


**Figure 3.** Comparison of the surface-based diameter distribution (IAT: Image Analysis Technique, LDT: Laser-Diffraction Technique)

This is particularly true for the results obtained with Inj. 1. For the second injector, the equality is acceptable for an injection pressure less than 10 bar. For greater injection pressures, the Sauter mean diameter  $\delta_{32}$  becomes less than  $3Ds_I$ . It must be said that, for these operating conditions (Inj. 2,  $\Delta P_i > 10$  bar), the LDT surface-based diameter distribution  $f_s(\delta)$  is not complete in the small diameter range. See for example the LDT distribution at 10 bar shown in Fig. 2. This is a consequence of the truncation performed in the small diameter range. For injection pressure greater than 10 bar, this truncation procedure affects the whole distribution too much and indicates that the Image Analyzing Technique is not accurate enough to catch the small drop population that represents a non negligible proportion of the distribution. However, for small injection pressure, both diagnostics are accurate enough to analyze the sprays and report a mean diameter  $\delta_{32}$  equal to  $3Ds_I$ . As explained when introducing the shape parameter series  $PF_m$  above (Eq. (3)), the mean diameter  $D'_{32}$  of a set of circular drops is equal to  $3Ds_I$ . The LDT reports a drop-diameter distribution. Therefore, this distribution characterizes a set of spherical droplets and the result showed in Fig. 4 indicates that the mean-scale  $Ds_I$  of the LDT drop-diameter distribution is equal to the mean-scale  $Ds_I$  of the actual spray. This observation encourages us to compare the scale distribution of the set of spherical drops characterized by the LDT distribution with the scale distribution of the actual spray.

Figure 5 shows the cumulative scale distributions obtained with Inj. 1 for all injection pressures. The LDT cumulative scale distributions were calculated with Eq. (4). This figure reports a rather good agreement between the cumulative scale distributions obtained with the two diagnostics. At low injection pressures, it is also found that the

We first compare the surface-based drop diameter distributions obtained from Image Analysis Technique (IAT) and from the Laser-Diffraction Technique (LDT), i.e.,  $f_s(D')$  and  $f_s(\delta)$ , respectively. The distribution  $f_s(\delta)$  is calculated from Eq. (4). This comparison is presented in Fig. 3 for Inj. 2 at two injection pressures. This figure immediately shows that the diameter  $\delta$  measured by the LDT is not identical to the equivalent-diameter  $D'$ . Indeed, the distributions  $f_s(D')$  extend over a larger diameter interval than  $f_s(\delta)$ . Similar results were obtained for the other operating conditions. The difference between  $f_s(D')$  and  $f_s(\delta)$  shown in Fig. 3 is of course related to the fact that droplets are not spherical since for spherical objects both distributions  $f_s(D')$  and  $f_s(\delta)$  should be the same.

In Fig. 4, the Sauter mean-diameter  $\delta_{32}$  of the LDT distribution is compared with three times the mean-scale  $Ds_I$ . This figure gathers the results obtained for all operating conditions. The linear regression plotted in this graph reports that  $\delta_{32}$  and  $3Ds_I$  are almost equal.

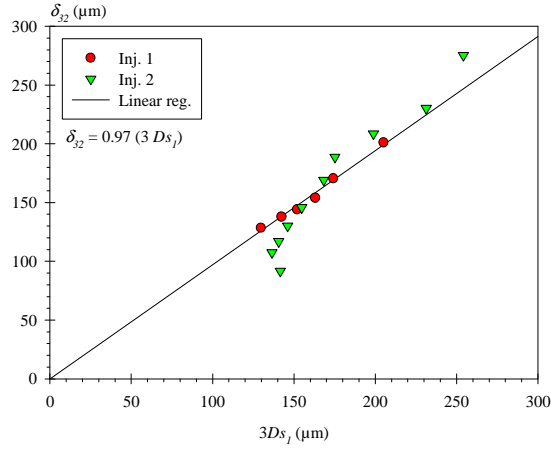


**Figure 4.** Comparison between  $\delta_{32}$  and  $3.Ds_1$  (all operating conditions)

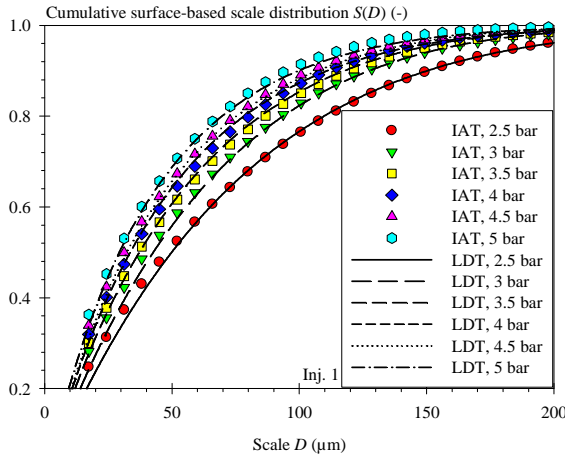


**Figure 5.** Comparison between the cumulative surface-based scale distributions  $S(D)$  (Inj. 1)

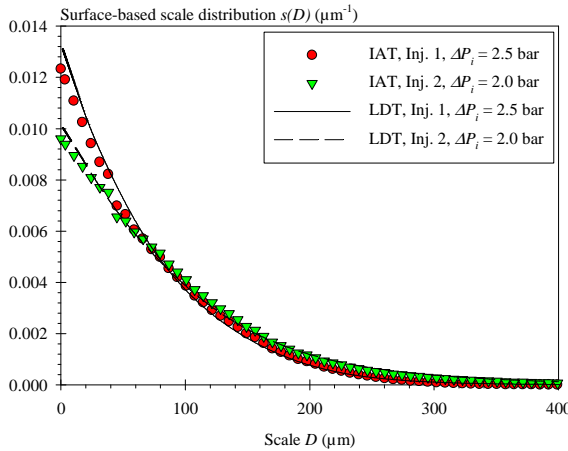


**Figure 6.** Comparison between the surface-based scale distribution  $s(D)$  (selected working conditions)

first derivative of the cumulative surface-based scale distributions, the scale distributions  $s(D)$  agree well with each other. Two examples are presented in Fig. 6. This result is important and induces the idea that the LDT reports the drop-diameter distribution of the set of spherical drops that has the same scale distribution as the actual spray. It can be demonstrated that the drop-diameter distribution of a set of spherical drops with a given scale distribution  $s(D)$  is unique. Indeed, a given scale distribution is characterized by a given mean-scale series  $Ds_n$ . The shape parameters  $PF_n$  of a spherical drop set being all equal to 1 whatever  $n$ , Eq. (3) reports a unique mean-diameter series, i.e., a unique drop-diameter distribution.

This result confirms that LDT distributions depend on the shape of the droplets and gives rise to the following question: how information related to the shape of the drops can be extracted from a LDT distribution? An answer to this question has been found in the analysis of the mean-diameter series  $\delta_{qp}$  of the LDT distribution and more specifically in the mean-diameter series  $\delta_{q2}$  as a function of  $q$ . Figure 7 shows this mean diameter series for Inj. 2 as a function of the injection pressure. In each case, the increase of the mean diameter with  $q$  follows a 2<sup>nd</sup> order polynomial evolution, i.e.:

$$\delta_{q2} = a_2 q^2 + a_1 q + a_0 \quad (5)$$

Similar behavior was observed for Inj. 1 and for both injectors, the 2<sup>nd</sup> order polynomial regression coefficient was always greater than 0.999. It can be noted in Fig. 7 that the parameter  $a_2$  introduced by Eq. (5) increases with the injection pressure. The Image Analysis Technique reported decreasing shape parameters  $PF_n$  when the injection pressure increases. This evolution indicates that the droplets, where they are measured, are less and less spherical as the injection pressure increases. These considerations on the influence of the injection pressure suggest investigating the relationship between the parameter  $a_2$  and the spray shape parameter. For all operating conditions (Inj. 1 and 2), Fig. 8 plots the parameter  $a_2$  versus the shape parameter  $PF_1$ . This figure clearly evidences a correlation between these two parameters. Although all the points seem to align, this specific linear behavior might be representative of the present working conditions. Further experimental work is required to discuss this very point. However, the behavior reported in Fig. 8 indicates that information on the shape of the droplets is available in the mean-diameter series of the LDT distribution: the greater  $a_2$ , the less spherical the drops are.

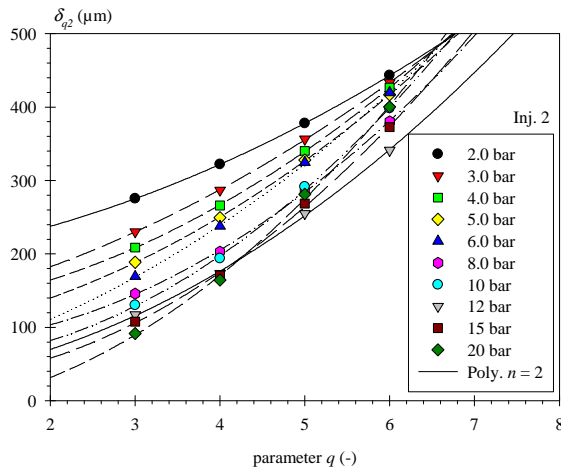


**Figure 7.** Mean diameter series  $\delta_{q2}$  versus  $q$  (Inj. 2)

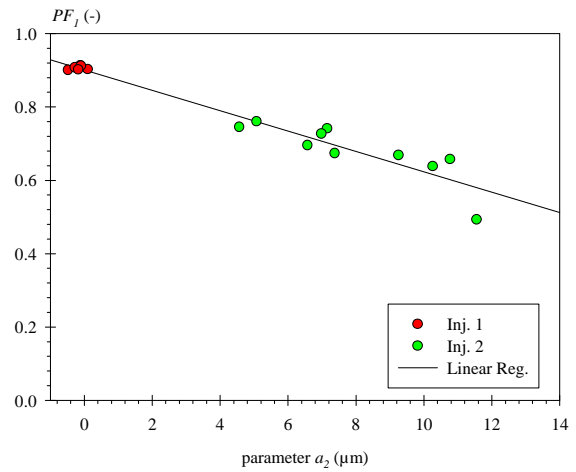


**Figure 8.** Shape parameter  $PF_1$  versus the parameter  $a_2$  (all operating conditions)

## Conclusion

This work shed more light on the definition of the drop-diameter distribution measured by a Laser-Diffraction Technique. The measurements conducted within the scope of this study clearly evidence dependence between the LDT drop-diameter distribution and the shape of the drops of the spray. To our knowledge, this dependence has never been experimentally reported or investigated in the past. The main conclusion of this work is that it has been demonstrated that the mean-diameter series of a LDT distribution contains information on the shape of the drops. By analyzing the mean-drop diameter series  $\delta_{q2}$  as a function of the parameter  $q$  allows sprays to be categorized according to the average shape of the droplets. This LDT performance has not been fully understood in this work. However it is believed that it is due to the fact that LDT performs a multi-scale description of the elements of the spray. This hypothesis that requires further work to be fully demonstrated is supported by the fact that the surface-based scale distribution of the LDT diameter distribution is very similar to the one of the actual spray. This result induces the idea that that LDT conserves the scale-distribution: it reports the diameter distribution of the set of spherical drops that has the same scale distribution of the actual spray. These results reveal LDT potentialities that deserve to be explored.

## References

1. Dodge, L.G., Rhodes, D.J. and Reitz, R.D., *Applied Optics*, 26:2144-2154 (1987).
2. Black, D.L., McQuay, M.Q., Bonin, M.P., *Prog. Energy Combust. Sci.*, 22:267-306 (1996)
3. Borovoi, A., Nats, E., Oppel, U. and Grishin, I., *Applied Optics*, 39:1989-1997 (2000)
4. Mühlenweg, H., Hirleman, E.D., *Part. Part. Syst. Charact.*, 15:163-169 (1998)
5. Dumouchel, C., Cousin, J. and Grout, S., *Journal of Flow Visualization and Image Processing*, 15:59-83 (2008).
6. Dumouchel, C., Grout, S. and Cousin, J., *ILASS-Europe Conference*, Como, Italy, September 2008, paper ID ILASS08-A091
7. Dumouchel, C., Cousin, J. and Triballier, K., *Experiment in Fluids*, 38:637-647 (2005)